Journal of Catalysis 279 (2011) 246–256

Contents lists available at ScienceDirect

Journal of Catalysis

journal homepage: www.elsevier.com/locate/jcat

Microcalorimetric adsorption studies of highly loaded Co–ZrO_2/SiO_2 catalysts for Fischer–Tropsch synthesis

Liang Chen, Jianyi Shen *

Laboratory of Mesoscopic Chemistry, School of Chemistry and Chemical Engineering, Nanjing University, Nanjing 210093, China

ARTICLE INFO

Article history:
Received 30 August 2010
Revised 12 January 2011
Accepted 15 January 2011
Available online 3 March 2011

Keywords:
Highly loaded Co/SiO_2 catalysts
ZrO_2 promoter
Fischer–Tropsch synthesis
Microcalorimetric adsorption
Sequential adsorption studies

ABSTRACT

Highly loaded Co/SiO_2 catalysts were prepared by a co-precipitation technique with an *n*-butanol drying process for Fischer–Tropsch synthesis (FTS). With the increase in cobalt loading from 20% to 80%, the FTS activity of the catalysts increased greatly. The addition of ZrO_2 improved the dispersion of cobalt and promoted the adsorption of H_2 and CO on cobalt. The preadsorbed H atoms significantly enhanced the adsorption of CO and C_2H_4, especially on cobalt promoted by ZrO_2. While the adsorption of C_2H_4 onto clean cobalt led to the formation of ethylidyne, π- and di-σ-bonded C_2H_4 might form on the CO-preadsorbed 80%Co/SiO_2 and 80%Co–8%ZrO_2/SiO_2, respectively. The presence of ZrO_2 strengthened the bonding of molecularly adsorbed ethylene and increased its uptake on CO-preadsorbed cobalt, which might be why the 80%Co–8%ZrO_2/SiO_2 exhibited such high activity for the hydrogenation of CO to heavy hydrocarbons.

1. Introduction

The reactions of Fischer–Tropsch synthesis (FTS) have been widely studied, because it provides a feasible route for the synthesis of clean fuels from syngas without any sulfur and aromatic compounds [1–3]. Co-based catalysts were found to exhibit high activity for producing linear heavy hydrocarbons with low activity for the water–gas shift reaction [4–6]. Previous studies [2,7–9] showed that the reducibility and dispersion of supported cobalt might be the important factors determining activity and selectivity to heavy hydrocarbons, and activity and C_5^+ selectivity were related to the number of metallic cobalt particles (larger than 7–8 nm) on the surface. Supported cobalt catalysts were usually prepared by the incipient wetness impregnation method [6,10–13] with porous materials such as alumina, silica, and active carbons as supports. When the loading of cobalt was low (e.g., lower than 30%), precursors of cobalt were highly dispersed on the supports. However, the strong interactions between the metal and supports led to the formation of compounds such as cobalt silicates and cobalt aluminates that were difficult to reduce [2,14–16], resulting in FTS catalysts with low activity, high selectivity to methane, and low selectivity to C_5^+.

Two methods are usually used to improve the activity of cobalt catalysts for FTS. One is to increase the loading of cobalt [10,17,18], so that more cobalt can be reduced and hopefully more active sites may be created. Thus, sol–gel and co-precipitation methods combined with a supercritical drying technique are usually used to prepare cobalt catalysts with high surface area and high loading and dispersion of supported cobalt. Another way is to add promoters to cobalt catalysts. Promoters such as Zr, La, Mn, Ce, and V were added and found to improve the reducibility and dispersion of supported Co [10,11,14,19–21]. In addition, some promoters retarded the deactivation and coke deposition of cobalt catalysts for FTS.

In this work, highly loaded Co/SiO_2 catalysts were prepared by the co-precipitation method with an *n*-butanol drying process so that the surface area of catalysts, as well as the reducibility and dispersion of supported cobalt, was significantly enhanced [22,23]. Accordingly, the catalysts were found to be highly active and selective to C_5^+ for the FTS. In addition, ZrO_2 was added as a promoter. Techniques such as X-ray diffraction (XRD), transmission electron microscopy (TEM), and microcalorimetric adsorption were used to characterize the catalysts, and efforts were made to correlate the FTS reactivity to the surface properties of catalysts.

The α-olefins and their adsorbed forms are believed to be important for carbon chain propagation during the FTS. It was reported that α-olefins such as ethylene could act as chain initiators and their readsorption would lead to further chain growth [1,24–27]. Girardon et al. [6] found that the cobalt catalysts that adsorbed more propylene exhibited higher activity and selectivity to C_5^+ in FTS. Ethylene is a simple olefin. The uptake of ethylene may reflect the chain propagation probability of a FTS catalyst. In addition, different reactants, intermediates, and products may adsorb simultaneously onto the cobalt surface and affect the subsequent adsorption and surface reactions. Although complete description

* Corresponding author. Fax: +86 25 83594305.
E-mail address: jyshen@nju.edu.cn (J. Shen).

0021-9517/$ - see front matter © 2011 Elsevier Inc. All rights reserved.
doi:10.1016/j.jcat.2011.01.014

of such mutual interactions is a tremendous task, the interactions of simple molecules such as H_2, CO, and ethylene on the surfaces of FTS catalysts may provide useful information about the surface properties that could be related to the initial reactivity of FTS catalysts.

2. Experimental

2.1. Preparation of catalysts

Co/SiO_2 catalysts containing about 20, 40, 60, and 80 wt.% cobalt were prepared by the co-precipitation method. $Co–ZrO_2/SiO_2$ catalysts with different amounts of ZrO_2 (2–12 wt.%) were prepared similarly. Specifically, desired amounts of metal nitrates ($Co(NO_3)_2{\cdot}6H_2O$ and/or $(Zr(NO_3)_4{\cdot}5H_2O$, both in AR grade) were dissolved in 100 ml distilled water to form a solution (I). Another solution (II) was obtained by dissolving desired amounts of Na_2CO_3 (AR) and $Na_2SiO_3{\cdot}9H_2O$ (AR) in 100 ml distilled water. The two solutions were simultaneously added dropwise into a beaker containing 250 ml distilled water at 353 K under vigorous stirring. The precipitates formed were filtered and washed thoroughly with water until the pH of the filtrate was 7. *n*-Butanol (about 200 ml, AR) was then added into a precipitate and heated at 353 K overnight, while water and *n*-butanol were evaporated. The powder samples were further dried in an oven at 393 K for 12 h. Then, they were pressed, crashed, and sieved to 20 and 40 meshes for further use.

2.2. Characterization of catalysts

The nitrogen adsorption/desorption isotherms were determined at 77 K using a Micromeritics Gemini V 2380 autosorption analyzer. Catalysts were usually outgassed in flowing nitrogen at 573 K for 3 h prior to the measurements. The specific surface areas were calculated using the Brunauer–Emmett–Teller (BET) method, and the pore size distributions were obtained according to the desorption branches by the Barrett–Joyner–Halenda (BJH) method.

XRD patterns were collected in ambient atmosphere by an X-ray diffractometer (Shimadzu XRD-6000) with Cu Kα radiation (λ = 1.5408 Å) generated at 40 kV and 30 mA. Diffraction intensities were recorded from 10° to 80° at a rate of 2.00°/min with a sampling width of 0.02°.

Temperature-programmed reduction measurements (TPR) were performed using a quartz U-tube reactor loaded with about 50 mg of a dried sample in 5.03% H_2/N_2 (V/V) at a flow rate of 40 ml/min. The hydrogen consumption was monitored by a thermal conductivity detector (TCD). The reducing gas first passed through the reference arm of the TCD before entering the reactor. The exiting gas passed through a trap filled with soda lime to remove water and possibly CO_2 and then reached the second arm of the TCD.

Microcalorimetric adsorption measurements were performed using a Tian–Calvet Type C-80 microcalorimeter (Setaram, France), which was connected to a glass vacuum-dosing system, equipped with a Baratron capacitance manometer (USA) for pressure measurement and gas handling. About 0.1 g of catalyst was loaded, reduced at 773 K for 2.5 h in flowing H_2, and then evacuated at 773 K for 1 h prior to measurement. Then, the microcalorimetric adsorption of CO, H_2, C_2H_4, NH_3, and CO_2 was carried out. In addition, two different probe gases were adsorbed successively onto the reduced $80\%Co/SiO_2$ and $80\%Co–8\%ZrO_2/SiO_2$. For example, the microcalorimetric adsorption of CO was first performed at 303 K on the reduced $80\%Co/SiO_2$, followed by evacuation at 303 K for 3 h to remove the weakly adsorbed CO molecules. Then, another probe molecule such as ethylene was dosed onto the catalyst at 303 K to measure the heat of adsorption of ethylene on the catalyst with CO preadsorbed, and vice versa. In this way, pairs of gases such as H_2/CO, CO/ethylene, and H_2/ethylene were studied by the microcalorimetric adsorption. The catalysts were usually evacuated at 303 K for 3 h before the second probe gas was adsorbed. The situation of adsorption of CO followed by the adsorption of ethylene on $80\%Co/SiO_2$ was expressed as $C_2H_4/CO/80\%Co/SiO_2$. In contrast, the adsorption of ethylene followed by CO on $80\%Co/SiO_2$ could be expressed as $CO/C_2H_4/80\%Co/SiO_2$.

The infrared (IR) spectra were recorded on a Bruker VERTEX 70 spectrometer with an MCT detector (in the range of 1000–4000 cm^{-1}). A catalyst (about 20 mg) was pressed into a self-supporting pellet and loaded into an in situ IR cell. It was reduced in H_2 at 773 K for 2.5 h, followed by evacuation at 773 K for 1 h. After cooled down to 303 K, certain amount of CO and C_2H_4 (about 4 kPa) was introduced subsequently into the IR cell and kept for 1 h. Then, the IR cell was evacuated for 1 h to remove gaseous molecules. The IR spectra were collected before and after the introduction of adsorbates. For the adsorption of C_2H_4 on the CO-preadsorbed samples, CO was adsorbed and evacuated at 303 K and an IR spectrum was then collected as background before the introduction of C_2H_4.

The adsorption of H_2 and O_2 was carried out in a homemade volumetric apparatus. The catalysts were reduced in H_2 at 773 K for 4 h and evacuated at 773 K for 1 h before the measurements. The adsorption of H_2 was performed at 423 K [28,29]. After the adsorption of H_2, the sample was heated to 673 K at a rate of 10 K/min and evacuated at the temperature for 1 h. The adsorption of O_2 was then performed at 673 K. The uptake of H_2 and O_2 was obtained by extrapolating the coverage of corresponding isotherms to $P = 0$. The degree of reduction (reducibility), dispersion, and average particle size of supported cobalt were calculated based on the amounts of H_2 and O_2 adsorbed and the loading of cobalt. The detailed calculation formulas could be found in the literature [30].

2.3. Catalytic tests

Reactions of FTS were carried out in a fixed bed reactor. The reactor consisted of a stainless steel tube with an internal diameter of 10 mm heated by an electronic oven. Syngas was regulated with a mass flow controller. The reaction pressure was maintained by a back-pressure regulator. Typically, 3 g of catalyst mixed with quartz sands was loaded into the reactor. Prior to the reaction, the catalyst was reduced at 773 K in flowing H_2 (30 ml/min) for 4 h under atmospheric pressure. After the temperature was lowered to 373 K, syngas (H_2:CO:N_2 = 64:32:4 mol ratio) was introduced, and the reactor was heated to the desired reaction temperatures. N_2 was added as an internal standard for the analysis of CO and products by a gas chromatograph (GC).

A hot trap at 423 K and a cold trap at 273 K were used to collect wax and liquid products, respectively. The FTS reactions reached steady state on the catalysts after 12 h, and the effluent gases from the traps were analyzed on line by a GC. A TDX-01 column was used with a TCD for the analysis of gaseous products CO, N_2, CO_2, and CH_4, while a Porapak-Qs column with a flame ionization detector (FID) was employed for the analysis of light hydrocarbons (C_1–C_4). Wax and liquid products were not analyzed, but were weighed. The conversion of CO and selectivity of different products were calculated according to the following equations:

$$\text{Conversion of CO } (\%) = \frac{n_{\text{CO,inlet}} - n_{\text{CO,outlet}}}{n_{\text{CO,inlet}}} \times 100\%$$

$$\text{Selectivity to } CO_2 \ (\%) \frac{n_{CO_2,\text{produced}}}{n_{\text{CO,inlet}} - n_{\text{CO,outlet}}} \times 100\%$$

$$\text{Selectivity to } CH_4\ (\%) = \frac{n_{CH_4,\text{produced}}}{n_{CO,\text{inlet}} - n_{CO,\text{outlet}} - n_{CO_2,\text{produced}}} \times 100\%$$

$$\text{Selectivity to } C_2 \sim C_4\ (\%) = \frac{n_{C_2\sim C_4,\text{produced}}}{n_{CO,\text{inlet}} - n_{CO,\text{outlet}} - n_{CO_2,\text{produced}}} \times 100\%$$

$$\text{Selectivity to } C_5^+\ (\%) = 1 - S_{CH_4} - S_{C_2} - S_{C_3} - S_{C_4}$$

3. Results and discussion

3.1. Catalytic performance

Table 1 shows the results of FTS for Co/SiO_2 catalysts with different cobalt loadings. With the increase in cobalt loading from 20% to 80%, the conversion of CO increased greatly from 7% to 100% at 483 K and 2 MPa while the selectivity to CO_2 decreased from 6.2% to 2.4%. The selectivity to C_5^+ was maintained around 83–90% with the increased loading of Co. The activity of 80%Co/SiO_2 was particularly high, since the conversion of CO almost reached 100% even at 473 K, with low selectivity to CO_2 (1.8%) and high selectivity to C_5^+ (89%).

Different amounts of ZrO_2 were added to the 80%Co/SiO_2 by the co-precipitation method. The FTS reactions were performed at 463 K and 2 MPa for the 80%Co–ZrO_2/SiO_2 catalysts. The results are summarized in Table 2. It is seen that the 80%Co/ZrO_2 exhibited 28.9% convention of CO and 86.8% selectivity to C_5^+, respectively; both were lower than for 80%Co/SiO_2 (79.5% and 91.5%, respectively). Thus, the activity of 80%Co/ZrO_2 was quite low for FTS. However, addition of ZrO_2 as a promoter into the 80%Co/SiO_2 made a great difference. The data in Table 2 show that with the increase in ZrO_2 from 0% to 8%, the conversion of CO increased from 79.5% to 92%. Meanwhile, the selectivity to C_5^+ was increased from 91% to 95% with the decreased selectivity to CH_4. However, excessive addition of ZrO_2 (such as 12%ZrO_2) decreased the conversion of CO and selectivity to C_5^+. In fact, the 80%Co–12%ZrO_2/SiO_2 showed some behavior of the 80%Co/ZrO_2 for FTS reactions, since only 8% SiO_2 was contained in it. Thus, the addition of the proper amount of ZrO_2 (e.g., 8%) promoted the conversion of CO and enhanced the selectivity to C_5^+ for FTS over the Co–ZrO_2/SiO_2 catalysts.

Based on the above results, we selected four catalysts (80%Co/SiO_2, 80%Co–4%ZrO_2/SiO_2, 80%Co–8%ZrO_2/SiO_2, and 80%Co/ZrO_2) for further studies to understand the effect of ZrO_2 on the surface properties of Co/SiO_2 catalysts.

Table 1
Catalytic performance of Co/SiO_2 catalysts with different cobalt loadings in FTS reactions (P = 2 MPa and GHSV = 500 ml/(g_{catal} h)).

Catalyst	T (K)	Conversion (%)	Selectivity (%)			
			CO_2	CH_4	C_2–C_4	C_5^+
20%Co/SiO_2	483	7.0	6.2	9.2	1.3	89.5
40%Co/SiO_2	483	45.7	8.1	7.1	7.0	85.9
60%Co/SiO_2	473	83.2	2.6	9.7	3.4	86.9
	483	99.2	5.7	10.0	2.8	87.2
80%Co/SiO_2	473	99.3	1.8	8.4	2.7	88.9
	483	100	2.4	13.1	3.5	83.4

Table 2
Catalytic performance of 80%Co–ZrO_2/SiO_2 catalysts with different ZrO_2 loadings for the FTS reactions (P = 2 MPa, GHSV = 500 ml/(g_{catal} h), and T = 463 K).

Catalyst	Conversion (%)	Selectivity (%)			
		CO_2	CH_4	C_2–C_4	C_5^+
80%Co/SiO_2	79.5	0.2	5.1	3.4	91.5
80%Co–2%ZrO_2/SiO_2	82.7	2.7	2.7	1.6	95.7
80%Co–4%ZrO_2/SiO_2	83.9	1.6	2.9	2.0	95.0
80%Co–6%ZrO_2/SiO_2	87.4	3.0	2.7	2.4	94.9
80%Co–8%ZrO_2/SiO_2	91.9	2.7	3.0	2.0	95.0
80%Co–12%ZrO_2/SiO_2	54.3	2.4	6.8	4.0	89.2
80%Co/ZrO_2	28.9	0	9.4	3.8	86.8

3.2. Textural and structural properties of catalysts

Table 3 shows the surface areas and pore parameters for the four selected catalysts (80%Co/SiO_2, 80%Co–4%ZrO_2/SiO_2, 80%Co–8%ZrO_2/SiO_2, and 80%Co/ZrO_2) after the FTS reactions. The data showed that the 80%Co/SiO_2 possessed higher surface area, but smaller pore size, than the 80%Co/ZrO_2. Addition of ZrO_2 decreased the surface area, but increased the pore size. Thus, the pore parameters (in terms of surface area and pore size) of 80%Co–ZrO_2/SiO_2 were similar to those of 80%Co/ZrO_2. The increase in the pore size upon the addition of ZrO_2 might favor the diffusion of CO and H_2 in pores filled with liquid products as well as the diffusion of heavy hydrocarbons out of catalyst pores [2,31].

Because of the high activity and C_5^+ selectivity of these catalysts, the pores were usually filled with liquid products, and thus reduced cobalt species were more or less protected from oxidation when they were exposed to air. Fig. 1 shows the XRD patterns for the catalysts after FTS reactions. Two diffraction peaks at 21.3° and 23.7° are clearly seen for wax in the catalysts. A diffraction peak at 44.4° for metallic Co was observed for all the catalysts. The width of this diffraction peak was used to estimate the average sizes of supported cobalt particles according to the Scherrer equation (see Table 4). The cobalt particle sizes in the 80%Co/SiO_2 and 80%Co/ZrO_2 were found to be about 16 and 18 nm, respectively, while they were about 10 nm in the two Co–ZrO_2/SiO_2 catalysts. Thus, the addition of ZrO_2 improved the dispersion of Co on SiO_2. XRD results indicated that cobalt existed mainly as Co_3O_4 before the reduction (data not given). Only traces of Co_3O_4 were observed in the catalysts after the FTS reactions, which might be formed from the oxidation of some metallic Co in air. A diffraction peak

Table 3
Texture properties of selected catalysts after FTS reactions at 463 K.

Catalyst	BET area (m^2/g)	Pore volume (cm^3/g)	Average pore diameter (nm)
80%Co/SiO_2	81	0.4	11.7
80%Co–4%ZrO_2/SiO_2	33	0.2	17.4
80%Co–8%ZrO_2/SiO_2	38	0.3	19.4
80%Co/ZrO_2	36	0.2	21.1

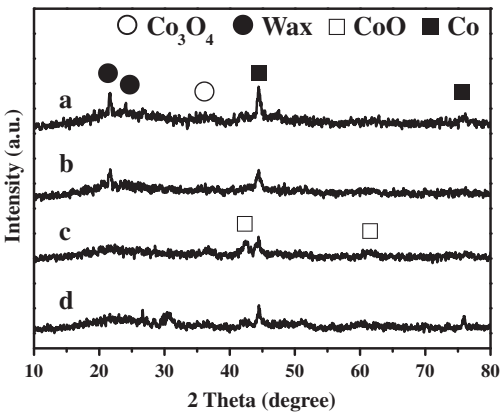

Fig. 1. XRD patterns of 80%Co/SiO_2 (a), 80%Co–4%ZrO_2/SiO_2 (b), 80%Co–8%ZrO_2/SiO_2 (c), and 80%Co/ZrO_2 (d) after FTS reactions at 463 K.

Table 4
Results of chemisorption of H_2 and O_2 on the selected catalysts reduced at 773 K with the sizes of supported Co particles determined by different methods.

Catalyst	Adsorption (μmol/g)		Dis.[a] (%)	Red.[b] (%)	Diam. of Co[c] (nm) by		
	H_2	O_2			XRD	H_2 ads.	TEM
80%Co/SiO_2	80	5184	2	57	16	46.5	48
80%Co–4%ZrO_2/SiO_2	164	4059	5	44	11	17.9	25
80%Co–8%ZrO_2/SiO_2	183	4212	6	46	10	16.4	20
80%Co/ZrO_2	97	6210	2	68	18	46.4	Hard to judge

[a] Dis. = dispersion.
[b] Red. = reducibility.
[c] Diam. = diameter.

at 42.4° for CoO was also observed for the 80%Co–8%ZrO_2/SiO_2 and 80%Co/ZrO_2, which might be due to the incomplete reduction of cobalt species in the catalysts. In fact, O_2 adsorption showed that only part of the supported cobalt was reduced to the metallic state.

TEM images of the four selected catalysts after FTS reactions are shown in Fig. 2. Small dispersed cobalt particles were observed in the 80%Co/SiO_2, with some large ones (see Fig. 2a), and the average size of the cobalt particles was estimated to be about 48 nm for the catalyst. Addition of 8%ZrO_2 changed the size distribution of cobalt particles and the sizes of cobalt particles became even (see Fig. 2c). The average size of cobalt particles was then estimated to be about 20 nm for the 80%Co–8%ZrO_2/SiO_2, close to that determined by H_2 adsorption (16.4 nm). Addition of 4%ZrO_2 led to a similar change in the size distribution of cobalt particles in 80%Co–4%ZrO_2/SiO_2 (see Fig. 2b), but the sizes of cobalt particles were not as even as in the 80%Co–8%ZrO_2/SiO_2. The average size of cobalt particles was estimated to be about 25 nm for the 80%Co–4%ZrO_2/SiO_2. No clear cobalt particles could be observed in the 80%Co/ZrO_2 (Fig. 2d), and thus the average particle size could not be estimated from its TEM image.

The number of surface cobalt sites could be titrated by the adsorption of H_2 at 423 K, according to which the average particle sizes of cobalt could be calculated. Table 4 summarizes the sizes of cobalt particles determined by XRD, TEM, and H_2 adsorption. The inconsistent results seem to indicate the limitations of different methods for the determination of particle sizes of Co [16]. However, the cobalt particle sizes in these catalysts determined by TEM and H_2 adsorption were quite close. Since only certain crystal faces of cobalt were collected by XRD, the average sizes of cobalt particles estimated by the Scherrer equation might be smaller.

3.3. Reducibility and dispersion of supported cobalt

Fig. 3 shows the TPR profiles for the four catalysts. Two main reduction peaks were observed for all four catalysts, which might be attributed to sequential reduction from Co_3O_4 to CoO and then to Co [11,12,32]. Thus, the addition of ZrO_2 did not change the reduction sequence of cobalt species. However, the second TPR peak seemed to shift to higher temperatures upon the addition of ZrO_2, indicating that the presence of ZrO_2 increased the interaction of cobalt species with the support.

The adsorption of H_2 and O_2 onto the reduced catalysts was carried out at 423 and 673 K, respectively, from which the dispersion and reducibility of supported cobalt could be derived. Table 4 summarizes the information obtained by the adsorption of H_2 and O_2. The data in Table 4 showed that the H_2 uptake increased from

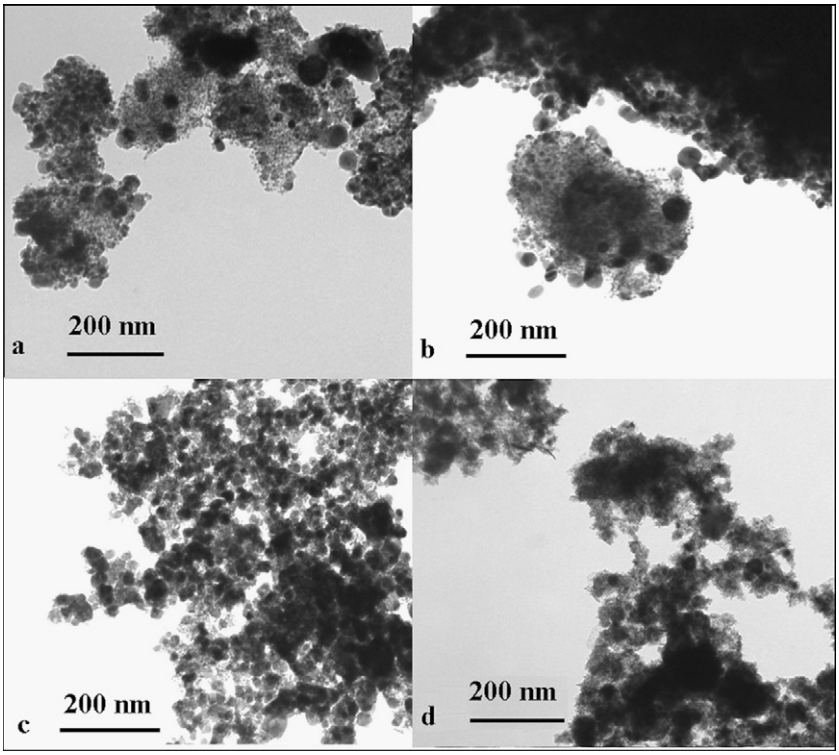

Fig. 2. TEM images of 80%Co/SiO_2 (a), 80%Co–4%ZrO_2/SiO_2 (b), 80%Co–8%ZrO_2/SiO_2 (c), and 80%Co/ZrO_2 (d) after FTS reactions at 463 K.

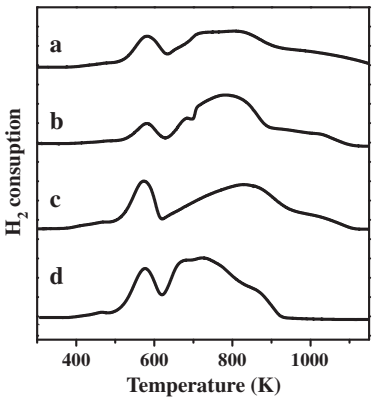

Fig. 3. TPR profiles of 80%Co/SiO_2 (a), 80%Co–4%ZrO_2/SiO_2 (b), 80%Co–8%ZrO_2/SiO_2 (c), and 80%Co/ZrO_2 (d) dried at 393 K.

80 μmol/g for the 80%Co/SiO_2 to 183 μmol/g for the 80%Co–8%ZrO_2/SiO_2, corresponding to the increase in cobalt dispersion from 2% to 6%. Meanwhile, the oxygen uptake was decreased, corresponding to the decrease in reduction degree (reducibility) from 57% to 46%. Thus, the addition of ZrO_2 increased the dispersion, while it decreased the reducibility of cobalt supported on SiO_2, consistent with the results of TEM and TPR. However, the increase in dispersion was much greater than the decrease in reducibility for supported Co, so that the number of active surface Co atoms was significantly increased upon the addition of ZrO_2.

3.4. Microcalorimetric adsorption of H_2 and CO

Apparently, the adsorption of CO and H_2 is important for FTS reactions. Thus, microcalorimetric adsorption of H_2 and CO onto the four selected catalysts was performed. Fig. 4a shows the results for microcalorimetric adsorption of H_2 at 423 K for the catalysts. The initial heat was about 73 kJ/mol for H_2 adsorption onto the 80%Co/SiO_2, which was increased to 83 kJ/mol when 8%ZrO_2 was added. The initial heat was about 90 kJ/mol for H_2 adsorption onto the 80%Co/ZrO_2, indicating that the Co–H bond was strengthened with the addition of ZrO_2. The uptake of H_2 was also increased upon the addition of ZrO_2.

Fig. 4b shows the results of microcalorimetric adsorption of CO at 298 K for the catalysts. The initial heat was about 90 kJ/mol for the adsorption of CO onto the 80%Co/SiO_2, which was increased to 93 kJ/mol when 8%ZrO_2 was added. The initial heat was also about 93 kJ/mol for CO adsorption onto the 80%Co/ZrO_2. The uptake of CO increased significantly from 101 μmol/g on the 80%Co/SiO_2 to 200 μmol/g on the 80%Co–8%ZrO_2/SiO_2.

These results showed that the uptake for the adsorption of H_2 and CO onto the supported cobalt was increased upon the addition of ZrO_2. However, the increase in uptake upon the addition of ZrO_2 was different for the adsorption of H_2 and CO, resulting in a change in the CO/H ratio adsorbed onto cobalt. The CO/H ratio was about 0.38 for the 80%Co/SiO_2, while it increased to about 0.56 on the 80%Co/ZrO_2 and Co–ZrO_2/SiO_2 catalysts, indicating that the addition of ZrO_2 enhanced the adsorption of CO more than that of H_2. CO could be adsorbed onto cobalt in linear or bridged forms. Thus, the adsorbed CO/H ratio should be between 0.5 (for bridged adsorption of CO) and 1 (for linear adsorption of CO). The CO/H ratio close to 0.5 suggested that CO was mainly adsorbed in bridged form on the catalysts. This was confirmed by the IR spectra for the adsorbed CO on the 80%Co/SiO_2, 80%Co–8%ZrO_2/SiO_2, and 80%Co/ZrO_2, as shown in Fig. 5. Two broad bands around 1870 and 1990 cm^{-1} were observed for the adsorption of CO on the catalysts,

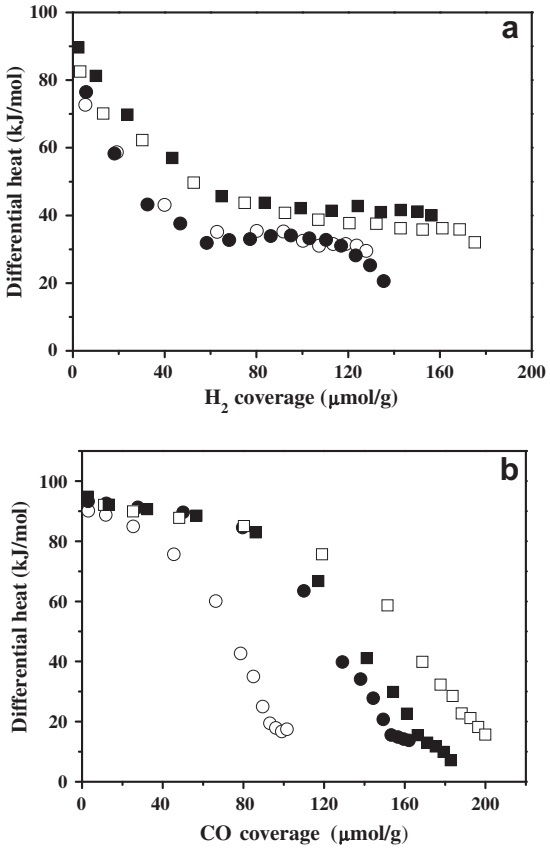

Fig. 4. Differential heat vs. coverage for the adsorption of H_2 at 423 K (a) and CO at 298 K (b) over 80%Co/SiO_2 (○), 80%Co–4%ZrO_2/SiO_2 (●), 80%Co–8%ZrO_2/SiO_2 (□), and 80%Co/ZrO_2 (■).

which can be attributed to the bridged [32–34] and linear adsorbed CO [33,35,36], respectively. Obviously, the band of bridged species (1870 cm^{-1}) was significantly more intensive than that of linear species (1990 cm^{-1}).

Since the addition of ZrO_2 enhanced the adsorption of H_2 and CO onto the surface of Co/SiO_2 in terms of both initial heat and uptake, the addition of ZrO_2 significantly enhanced the conversion of CO and selectivity to C_5^+ on the 80%Co–ZrO_2/SiO_2 catalysts for FTS reactions.

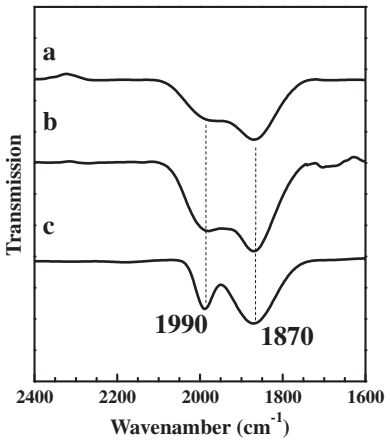

Fig. 5. Infrared spectra for the adsorption of CO at 303 K onto 80%Co/SiO_2 (a), 80%Co–8%ZrO_2/SiO_2 (b), and 80%Co/ZrO_2 (c). The catalysts were reduced and evacuated at 773 K before the adsorptions.

3.5. Surface acidic and basic properties

Previous studies revealed that the surface acid–base properties affected the activity and selectivity of FTS reactions significantly [24,37–39]. Cobalt oxides may interact strongly with acidic supports, leading to lowered reducibility of supported cobalt and thus low FTS activities. In addition, some acid-catalyzed reactions such as oligomerization, isomerization, and cracking might occur on strongly acidic sites, leading to coke deposition and inhibition of chain propagation of hydrocarbons [40,41]. On the other hand, the FTS activities of cobalt catalysts were significantly decreased when basic promoters such as K and Mg were added [10,24,42]. Thus, special attention should be paid to the change in surface acidic and basic properties of Co/SiO_2 catalysts upon the addition of ZrO_2.

Microcalorimetric adsorption of NH_3 and CO_2 was used to probe the surface acid–base properties of catalysts. Fig. 6a shows the results for the adsorption of ammonia at 423 K onto the catalysts reduced and evacuated at 773 K. The initial heat and uptake were measured to be about 83 kJ/mol and 500 μmol/g, respectively, on the $80\%Co/SiO_2$, while they were 111 kJ/mol and 350 μmol/g, respectively, on the $80\%Co/ZrO_2$, for the adsorption of ammonia. The higher initial heat indicated stronger surface acidity on $80\%Co/ZrO_2$ than on $80\%Co/SiO_2$. The lower uptake of ammonia on $80\%Co/ZrO_2$ might be due to the lower surface area of $80\%Co/ZrO_2$ than of $80\%Co/SiO_2$. The addition of ZrO_2 increased the initial heat of ammonia adsorption, indicating increased surface acidity of $Co–ZrO_2/SiO_2$ when compared to the Co/SiO_2. However, the surface acidity of the $80\%Co/ZrO_2$ did not seem to be strong enough to catalyze the cracking reactions of heavy hydrocarbons.

The results of microcalorimetric adsorption of CO_2 at 423 K on the reduced catalysts are shown in Fig. 6b. The initial heat and uptake were measured to be about 82 kJ/mol and 42 μmol/g, respectively, for the adsorption of CO_2 onto the $80\%Co/ZrO_2$. Thus, the $80\%Co/ZrO_2$ possessed some surface basicity. Thus, the surface of Co/ZrO_2 was both acidic and basic owing to the amphoteric properties of ZrO_2. Surprisingly, the uptake was very low and no heat was measured for the adsorption of CO_2 onto the $80\%Co–8\%ZrO_2/SiO_2$, indicating that the $80\%Co–ZrO_2/SiO_2$ catalysts essentially did not possess any surface basicity. Bouarab et al. [43] and López et al. [44] found that the addition of MgO increased the surface basicity of SiO_2-supported metal catalysts, and the increase in surface basicity was unfavorable for the FTS reactions [10,24,42]. Thus, ZrO_2 seemed a unique promoter that increased the surface acidity of Co/SiO_2 catalysts without affecting their surface basicity.

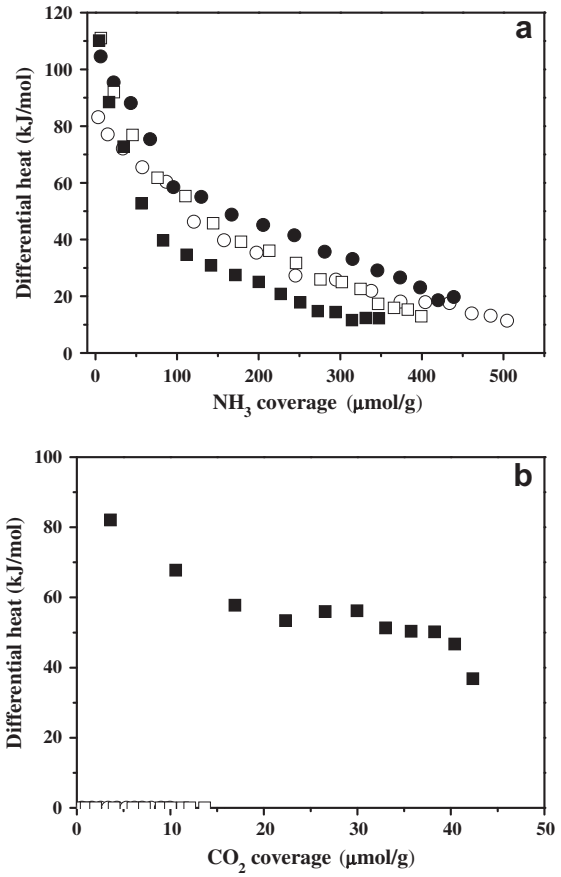

Fig. 6. Differential heat vs. coverage for NH_3 (a) and CO_2 (b) adsorption over $80\%Co/SiO_2$ (○), $80\%Co–4\%ZrO_2/SiO_2$ (●), $80\%Co–8\%ZrO_2/SiO_2$ (□), and $80\%Co/ZrO_2$ (■) reduced at 773 K. The microcalorimetric adsorption measurements were performed at 423 K.

3.6. Sequential adsorption studies

3.6.1. Sequential adsorption of H_2 and CO

Studies showed that the adsorption of H_2 on cobalt was activated [28,29,45] and thus the heat of adsorption of H_2 was affected by the adsorption temperature. Fig. 7 shows the effect of temperature on the heat of H_2 adsorption on the $80\%Co/SiO_2$ and $80\%Co–8\%ZrO_2/SiO_2$ catalysts. The initial heat was about 57 and 73 kJ/mol for the adsorption of H_2 on the $80\%Co/SiO_2$ at 303 and 423 K, respectively. Greater initial heat was generated when the adsorption was performed at a higher temperature on the same catalyst, indicating that the adsorption of H_2 on cobalt needs activation energy. Surprisingly, the initial heat (70 kJ/mol) and uptake (247 μmol/g) were significantly increased for the adsorption of H_2 onto the $80\%Co–8\%ZrO_2/SiO_2$ at 303 K. The initial heat (70 kJ/mol) for the adsorption of H_2 at 303 K onto the $80\%Co–8\%ZrO_2/SiO_2$ was close to that (73 kJ/mol) for the adsorption of H_2 at 423 K onto the $80\%Co/SiO_2$, indicating that ZrO_2 promoted the dissociative adsorption of H_2 on the cobalt surface (i.e., lowered the activation energy for the adsorption of H_2 on Co). When H_2 was adsorbed at 423 K onto the $80\%Co–8\%ZrO_2/SiO_2$, the initial heat was further increased to 83 kJ/mol, while the uptake of H_2 was decreased from 247 to 175 μmol/g.

After the adsorption of H_2 at 303 and 423 K, respectively, onto the $80\%Co/SiO_2$ and $80\%Co–8\%ZrO_2/SiO_2$, the catalysts were evacuated at 303 K and the adsorption of CO was performed at 303 K. Fig. 8 shows the results. Generally, the desorption temperature (T_{des}) for the absorbed molecules was related to the adsorption

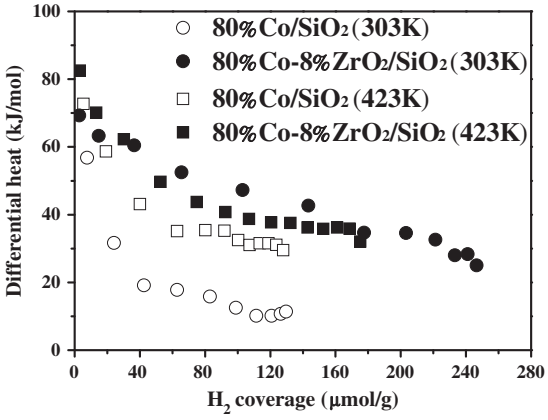

Fig. 7. Differential heat vs. coverage for H_2 adsorption over $80\%Co/SiO_2$ and $80\%Co–8\%ZrO_2/SiO_2$ at 303 and 423 K, respectively.

heat (ΔH_{ads}) of the adsorbed molecules by the equation $T_{des} = 4\Delta H_{ads}$, which stated that adsorbed molecules with adsorption heat lower than ΔH_{ads} could be desorbed at $T_{des} = 4\Delta H_{ads}$ [46,47]. Accordingly, the H_2 adsorbed onto the 80%Co/SiO_2 at 303 K (with the initial heat of 57 kJ/mol) might be almost completely desorbed when evacuating at 303 K, and those adsorbed on the 80%Co–8%ZrO_2/SiO_2 at 423 K (with the initial heat of 83 kJ/mol) could not be completely desorbed at 303 K.

Fig. 8a shows that the initial heat and coverage for the adsorption of CO on the clean 80%Co/SiO_2 at 303 K were about 90 kJ/mol and 87 μmol/g, respectively. After the adsorption of H_2 at 303 K followed by evacuation at 303 K, the adsorption of CO was performed again on the 80%Co/SiO_2, and initial heat and coverage similar to those for the clean catalyst were measured, indicating that all adsorbed H_2 was evacuated before the adsorption of CO in this case. However, after adsorption of H_2 at 423 K followed by evacuation at 303 K, the adsorption of CO onto the (H-preadsorbed) 80%Co/SiO_2 generated greater initial heat (96 kJ/mol) with greater coverage (171 μmol/g), indicating that the presence of preadsorbed H significantly enhanced the adsorption of CO onto the surface of cobalt. Since H is a strong electron donor [48], the presence of H increased the electron density in *d* orbitals of surface cobalt and thus increased the electron charges back-donated from *d* orbitals to the anti-bonding orbitals of adsorbed CO [49]. In this way, the Co–CO bonding was enhanced and more heat was generated for the adsorption of CO onto the Co surface with preadsorbed H atoms.

Fig. 8b shows the effect of preadsorbed H on the adsorption of CO onto the 80%Co–8%ZrO_2/SiO_2. Since the adsorption of H_2 was promoted by the presence of ZrO_2, some adsorbed H might remain on the surface of 80%Co–8%ZrO_2/SiO_2 after the adsorption of H_2 and then evacuation at 303 K. Accordingly, the heat and coverage of CO were higher (though not much, indicating that only a little H remained) on it than on the clean 80%Co–8%ZrO_2/SiO_2. After the adsorption of H_2 at 423 K followed by evacuation at 303 K, the adsorption of CO onto the H-preadsorbed 80%Co–8%ZrO_2/SiO_2 generated greater initial heat (101 kJ/mol) with greater coverage (287 μmol/g), indicating that the presence of preadsorbed H significantly enhanced the adsorption of CO on the surface of cobalt promoted by ZrO_2.

Since ZrO_2 promoted the adsorption of H_2 onto the surface of cobalt (both the initial heat and coverage of H_2 were increased), 80%Co–8%ZrO_2/SiO_2 was covered with more H atoms than 80%Co/SiO_2, after adsorption of H_2 and evacuation at 303 K. Accordingly, the adsorption of CO was more enhanced (in terms of uptake and surface bonding) on the H-preadsorbed surface of cobalt promoted by ZrO_2. Thus, ZrO_2 promoted not only the adsorption of H_2 and CO individually onto the clean surface of cobalt, but also the adsorption of CO particularly onto the H-preadsorbed surface of cobalt. While the initial heat and coverage were about 90 kJ/mol and 87 μmol/g, respectively, for the adsorption of CO at 303 K onto the clean 80%Co/SiO_2, they were found to be about 101 kJ/mol and 287 μmol/g, respectively, for the adsorption of CO at the same temperature onto the H-preadsorbed 80%Co–8%ZrO_2/SiO_2. Such a great difference in the adsorption of CO might account for the greatly positive effect of ZrO_2 as a promoter for Co/SiO_2 catalysts in the FTS reactions.

At 303 K, the heat of H_2 adsorption onto the 80%Co/SiO_2 was low (57 kJ/mol). The heat was significantly increased to 70 kJ/mol for the adsorption of H_2 at 303 K onto the 80%Co–8%ZrO_2/SiO_2. Thus, the effect of preadsorbed CO on the adsorption of H_2 onto 80%Co–8%ZrO_2/SiO_2 was more meaningful. The results are shown in Fig. 9. The initial heat and coverage were measured to be about 92 kJ/mol and 207 μmol/g, respectively, for the adsorption of CO at 303 K onto 80%Co–8%ZrO_2/SiO_2. After evacuation at 303 K, a large quantity of CO (more than 100 μmol/g) might remain on the surface of 80%Co–8%ZrO_2/SiO_2, which would definitely affect the adsorption of H_2. The initial heat and coverage were measured to be about 70 kJ/mol and 247 μmol/g, respectively, for the adsorption of H_2 onto the clean 80%Co–8%ZrO_2/SiO_2, while they were about 70 kJ/mol and 175 μmol/g, respectively, for the adsorption of H_2 onto the CO-preadsorbed 80%Co–8%ZrO_2/SiO_2. In addition, the heat was significantly decreased at coverage higher than 38 μmol/g for the adsorption of H_2 onto the CO-preadsorbed 80%Co–8%ZrO_2/SiO_2. Thus, the presence of CO inhibited the adsorption of H_2 on the surface of cobalt promoted by ZrO_2. Without the

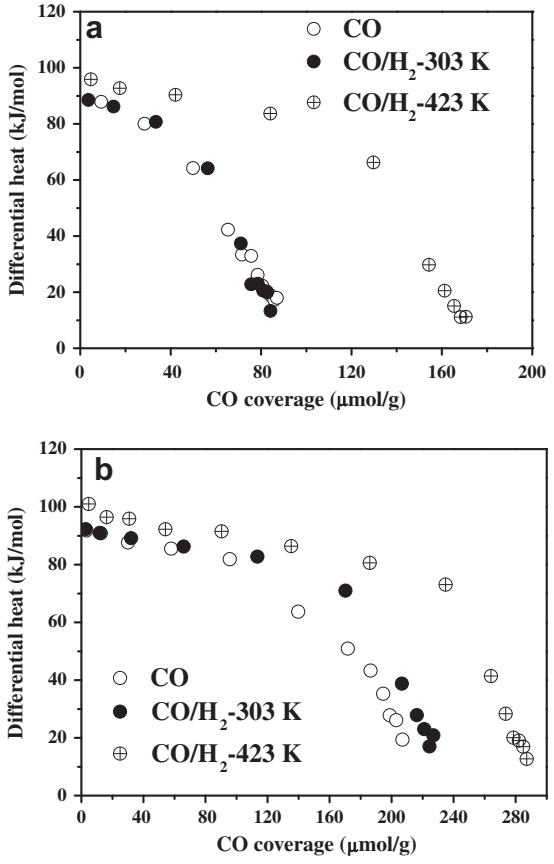

Fig. 8. Differential heat vs. coverage for CO adsorption onto clean and H_2-preadsorbed (CO/H_2) 80%Co/SiO_2 (a) and 80%Co–8%ZrO_2/SiO_2 (b) catalysts. The catalysts were reduced and evacuated at 773 K. After the adsorption of H_2 at 303 or 423 K and evacuation at 303 K, the microcalorimetric adsorption of CO was performed at 303 K (CO/H_2-303 K and CO/H_2-423 K).

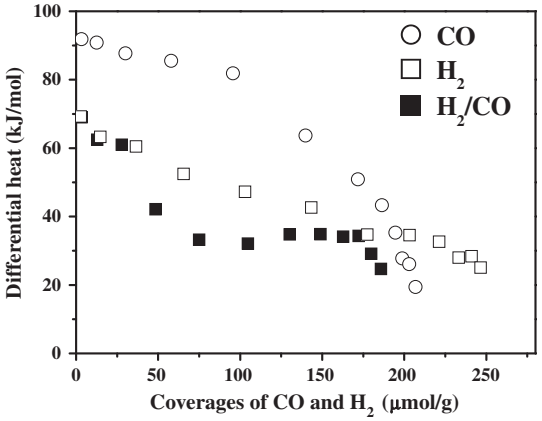

Fig. 9. Differential heat vs. coverage for H_2 adsorption onto clean and CO-preadsorbed (H_2/CO) 80%Co–8%ZrO_2/SiO_2. The catalyst was reduced and evacuated at 773 K. The microcalorimetric adsorption of CO and H_2 was performed at 303 K.

addition of ZrO_2, this inhibition effect was more profound for the adsorption of H_2 on the CO-preadsorbed 80%Co/SiO_2 (data not shown).

3.6.2. Sequential adsorption of H_2 and C_2H_4

Fig. 10 shows the results of microcalorimetric adsorption of C_2H_4 onto the clean and H-preadsorbed catalysts. The heat vs. coverage curve for the adsorption of C_2H_4 onto the surface of cobalt displayed a maximum due to the formation of surface ethylidyne species (CH_3–C≡) and H and the subsequent hydrogenation of C_2H_4 to ethane that was released to the gas phase [50,51]. Because of the generation of ethane during the adsorption of C_2H_4, the amount of C_2H_4 adsorbed as calculated volumetrically and thus the differential heat calculated by the heat released divided by the amount of C_2H_4 adsorbed were not accurate. In addition, the heat released due to the hydrogenation of ethylene also led to the overcalculation of adsorption heat. Thus, the heat and coverage presented in Fig. 10 for the adsorption of ethylene were nominal. However, the changes in heat and coverage for the adsorption of ethylene on the different catalysts were apparent.

Fig. 10a shows that the nominal initial heat and coverage were about 100 kJ/mol and 45 μmol/g, respectively, for the adsorption of C_2H_4 onto the clean 80%Co/SiO_2. The maximum on the heat vs. coverage curve was significantly enhanced for the adsorption of C_2H_4 on the H-preadsorbed 80%Co/SiO_2 with the preadsorption of H_2 at 303 K. The nominal heat and coverage were further enhanced for the adsorption of C_2H_4 on the H-preadsorbed 80%Co/SiO_2 with the preadsorption of H_2 at 423 K, indicating that the preadsorbed H promoted the dissociative adsorption of ethylene and the subsequent hydrogenation of adsorbed C_2H_4.

Fig. 10b shows that the nominal initial heat and coverage were about 100 kJ/mol and 90 μmol/g, respectively, for the adsorption of C_2H_4 onto the clean 80%Co–8%ZrO_2/SiO_2. When compared to the adsorption of C_2H_4 on the clean 80%Co/SiO_2, the dissociative adsorption and hydrogenation of ethylene were significantly enhanced with the presence of ZrO_2. The heat vs. coverage curves were similar for the adsorption of C_2H_4 onto the clean and H-preadsorbed 80%Co–8%ZrO_2/SiO_2 with the preadsorption of H_2 at 303 K. However, the nominal heat and coverage were greatly enhanced for the adsorption of C_2H_4 onto the H-preadsorbed 80%Co–8%ZrO_2/SiO_2 with the preadsorption of H_2 at 423 K. Comparing the results of adsorption of C_2H_4 onto the 80%Co/SiO_2 and 80%Co–8%ZrO_2/SiO_2 with preadsorbed H_2 at 423 K, it was apparent that the H-preadsorbed surface of cobalt in 80%Co–8%ZrO_2/SiO_2 was much more active than that in 80%Co/SiO_2 for the adsorption and hydrogenation of ethylene.

Fig. 11 shows the effect of preadsorbed C_2H_4 on the adsorption of H_2 onto the 80%Co–8%ZrO_2/SiO_2. The nominal initial heat and coverage were measured to be about 100 kJ/mol and 90 μmol/g, respectively, for the adsorption of C_2H_4 at 303 K onto the clean 80%Co–8%ZrO_2/SiO_2. After evacuation at 303 K, some ethylidyne and adsorbed ethylene must remain on the surface of 80%Co–8%ZrO_2/SiO_2. However, the presence of surface species from the adsorption of C_2H_4 at 303 K did not seem to affect the adsorption of H_2, since similar heat vs. coverage curves were obtained for the adsorption of H_2 onto the clean and C_2H_4-preadsorbed 80%Co–8%ZrO_2/SiO_2, as can be seen clearly in Fig. 11.

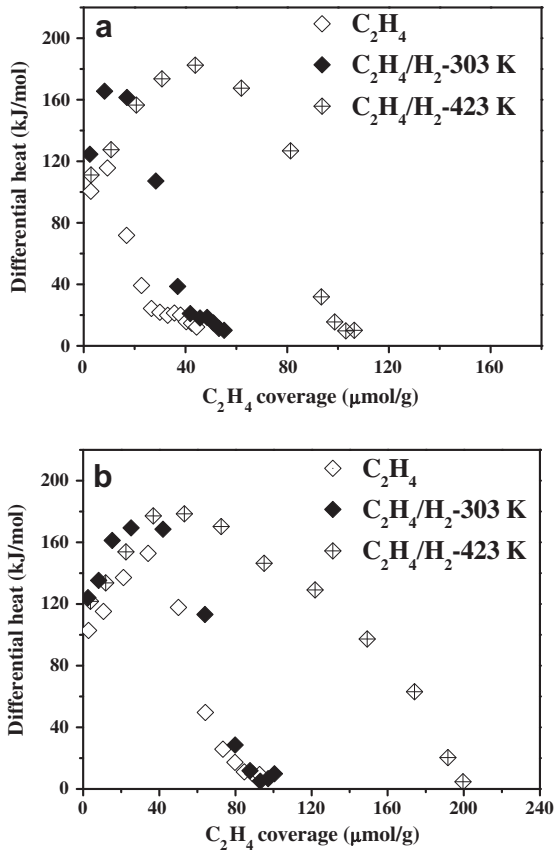

Fig. 10. Differential heat vs. coverage for ethylene adsorption onto clean and H_2-preadsorbed (C_2H_4/H_2) 80%Co/SiO_2 (a) and 80%Co–8%ZrO_2/SiO_2 (b) catalysts. The catalysts were reduced and evacuated at 773 K. After the adsorption of H_2 at 303 or 423 K and evacuation at 303 K, the microcalorimetric adsorption of ethylene was performed at 303 K (C_2H_4/H_2-303 K and C_2H_4/H_2-423 K).

3.6.3. Sequential adsorption of CO and C_2H_4

Fig. 12 shows the results of microcalorimetric adsorption of CO on the clean and C_2H_4-preadsorbed catalysts. Fig. 12a shows that the initial heat and coverage for the adsorption of CO onto the clean 80%Co/SiO_2 at 303 K were about 90 kJ/mol and 87 μmol/g, respectively. The initial heat was almost unchanged, while the coverage of CO was decreased to about 67 μmol/g, when CO was adsorbed onto the 80%Co/SiO_2 with C_2H_4 preadsorbed. Similarly, the initial heat and coverage for the adsorption of CO onto the clean 80%Co–8%ZrO_2/SiO_2 at 303 K were about 92 kJ/mol and 207 μmol/g, respectively. Again, the initial heat was almost unchanged, while the coverage of CO was decreased to about 122 μmol/g, when CO was adsorbed onto the 80%Co–8%ZrO_2/SiO_2 with C_2H_4 preadsorbed, as can be seen in Fig. 12b. These results indicated that the surface species such as ethylidyne formed from

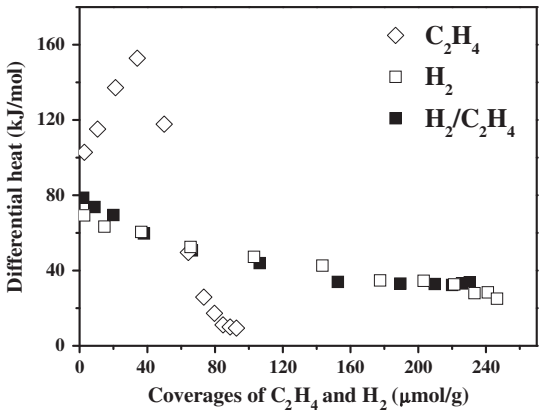

Fig. 11. Differential heat vs. coverage for H_2 adsorption onto clean and ethylene-preadsorbed (H_2/C_2H_4) 80%Co–8%ZrO_2/SiO_2. The catalyst was reduced and evacuated at 773 K. The microcalorimetric adsorption of ethylene and H_2 was performed at 303 K.

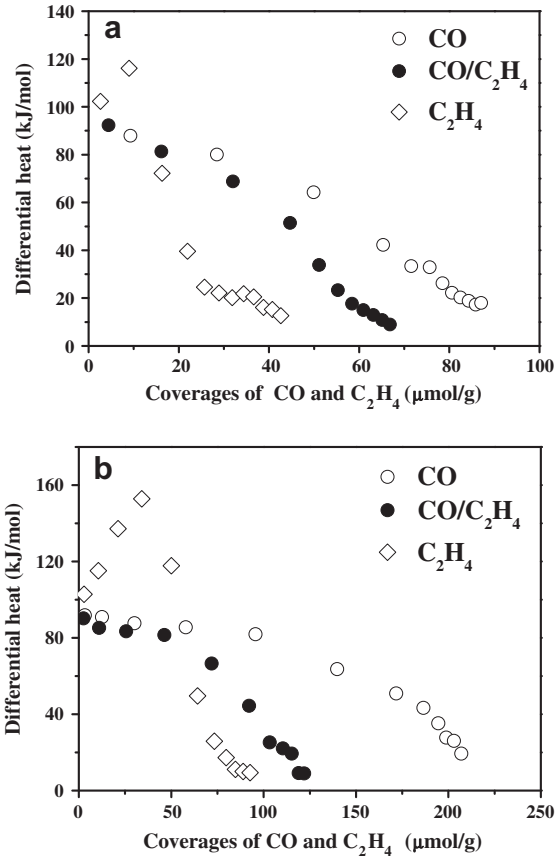

Fig. 12. Differential heats vs. coverage for CO adsorption onto clean and C_2H_4-preadsorbed (CO/C_2H_4) 80%Co/SiO_2 (a) and 80%Co–8%ZrO_2/SiO_2 (b) catalysts. The catalysts were reduced and evacuated at 773 K. The microcalorimetric adsorption of C_2H_4 and CO was performed at 303 K.

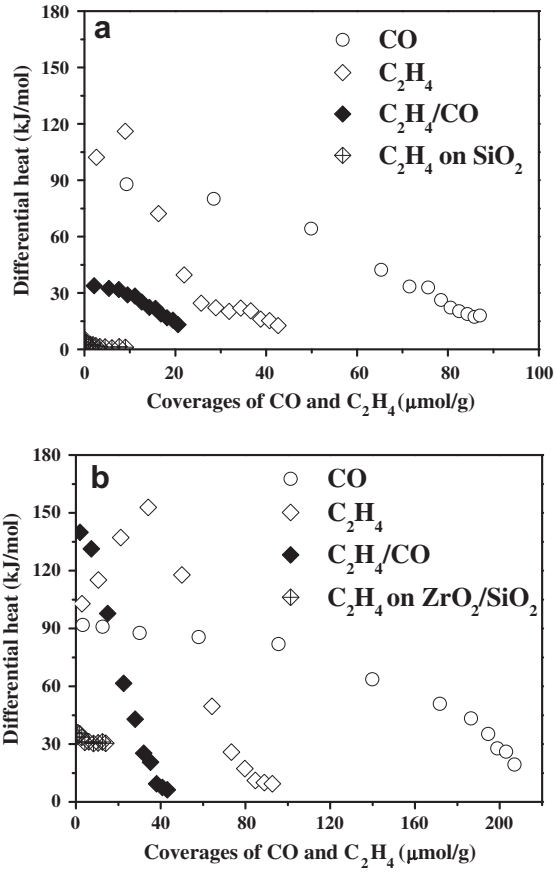

Fig. 13. Differential heats vs. coverage for C_2H_4 adsorption onto clean and CO-preadsorbed (C_2H_4/CO) 80%Co/SiO_2 (a) and 80%Co–8%ZrO_2/SiO_2 (b) catalysts. The catalysts were reduced and evacuated at 773 K. The microcalorimetric adsorption of CO and C_2H_4 was performed at 303 K. The adsorption of C_2H_4 onto SiO_2 and ZrO_2/SiO_2 is also presented for comparison.

the adsorption of C_2H_4 at 303 K occupied the surface cobalt sites in 80%Co/SiO_2 and 80%Co–8%ZrO_2/SiO_2 for the adsorption of CO.

The effect of preadsorbed CO on the adsorption of C_2H_4 onto the 80%Co/SiO_2 and 80%Co–8%ZrO_2/SiO_2 catalysts was studied and the results are shown in Fig. 13. Fig. 13a shows that the adsorption of C_2H_4 onto SiO_2 was negligible, and thus the possible effect of adsorption of C_2H_4 on the support could be excluded. According to the equation $T_{des} = 4\Delta H_{ads}$, about 30 μmol/g CO might remain on the surface of 80%Co/SiO_2 after adsorption of CO and then evacuation at 303 K. This was confirmed by the IR spectrum shown in Fig. 5a. Fig. 13a shows that the heat vs. coverage curves for the adsorption of ethylene onto the clean and CO-preadsorbed surfaces of 80%Co/SiO_2 were totally different. Both the initial heat and coverage for the adsorption of C_2H_4 onto the CO-preadsorbed 80%Co/SiO_2 were significantly decreased, and the heat maximum was no longer present on the heat vs. coverage curve. The initial heat and coverage were measured to be 34 kJ/mol and 21 μmol/g, respectively, for the adsorption of C_2H_4 onto the CO-preadsorbed 80%Co/SiO_2. The results indicated that the presence of preadsorbed CO inhibited the dissociative adsorption of C_2H_4. Because of the low adsorption heat (⩽34 kJ/mol), C_2H_4 must be adsorbed molecularly (or π-bonded) on the CO-preadsorbed surface of cobalt in the 80%Co/SiO_2 [50].

Fig. 13b shows that ZrO_2/SiO_2 adsorbed some C_2H_4 with heat lower than 40 kJ/mol. Apparently, this was due to the adsorption of C_2H_4 onto ZrO_2, since the adsorption of C_2H_4 onto SiO_2 was negligible. Thus, the presence of ZrO_2 might favor the adsorption of C_2H_4. The adsorption of C_2H_4 onto the clean 80%Co–8%ZrO_2/SiO_2 generated a heat vs. coverage curve with a heat maximum and nominal initial heat and coverage of about 102 kJ/mol and 93 μmol/g, respectively. On the other hand, the adsorption of C_2H_4 onto the CO-preadsorbed 80%Co–8%ZrO_2/SiO_2 was totally different. According to the equation $T_{des} = 4\Delta H_{ads}$, about 100 μmol/g CO might remain on the surface of 80%Co–8%ZrO_2/SiO_2 after adsorption of CO (see Fig. 13b) and then evacuation at 303 K. In fact, the IR bands of adsorbed CO on 80%Co–8%ZrO_2/SiO_2 were significantly more intensive than those on 80%Co/SiO_2, as can be seen from Figs. 5a and 5b. As mentioned above, the amount of CO that remained on the 80%Co/SiO_2 was about 30 μmol/g after evacuation at 303 K. The initial heat and coverage were measured to be about 140 kJ/mol and 45 μmol/g, respectively, for the adsorption of C_2H_4 onto the CO-preadsorbed 80%Co–8%ZrO_2/SiO_2 without a heat maximum. Thus, the presence of preadsorbed CO inhibited the dissociative adsorption of C_2H_4 onto the surface of Co promoted by ZrO_2. Notice the significant difference for the adsorption of C_2H_4 on the CO-preadsorbed 80%Co/SiO_2 and 80%Co–8%ZrO_2/SiO_2. While the initial heat and coverage were 34 kJ/mol and 21 μmol/g, respectively, for the adsorption of C_2H_4 onto the CO-preadsorbed 80%Co/SiO_2, they were 140 kJ/mol and 45 μmol/g, respectively, for the adsorption of C_2H_4 onto the CO-preadsorbed 80%Co–8%ZrO_2/SiO_2. Thus, the presence of ZrO_2 greatly promoted the adsorption of C_2H_4 onto the CO-preadsorbed cobalt sites. Because of the high initial adsorption heat (140 kJ/mol), C_2H_4 must be adsorbed mainly via di-σ bonding on the CO-preadsorbed surface of cobalt in 80%Co–8%ZrO_2/SiO_2 [50].

IR spectra were collected at 303 K for the adsorption of C_2H_4 onto the clean and CO-preadsorbed 80%Co/SiO_2 and

80%Co–8%ZrO_2/SiO_2 catalysts. Fig. 14 shows the results. A band around 1320 cm^{-1} was observed for the adsorption of C_2H_4 onto the clean 80%Co/SiO_2 and 80%Co–8%ZrO_2/SiO_2, which could be assigned to ethylidyne [50]. The band was more intensive for 80%Co–8%ZrO_2/SiO_2 than for 80%Co/SiO_2, indicating that more C_2H_4 was dissociatively adsorbed on 80%Co–8%ZrO_2/SiO_2 than on 80%Co/SiO_2. This band disappeared for the adsorption of C_2H_4 onto the CO-preadsorbed 80%Co/SiO_2 and 80%Co–8%ZrO_2/SiO_2, indicating the inhibition of dissociative adsorption of C_2H_4 for the formation of ethylidyne by the presence of adsorbed CO. Instead, a broad band around 1456 cm^{-1} was clearly seen for the adsorption of C_2H_4 onto the CO-preadsorbed 80%Co–8%ZrO_2/SiO_2, which could be attributed to di-σ-bonded ethylene [50]. This band was absent for the adsorption of C_2H_4 onto the CO-preadsorbed 80%Co/SiO_2. In addition, other bands were hardly observed for the adsorption of C_2H_4 on the CO-preadsorbed 80%Co/SiO_2. Thus, it may be inferred that only π-bonded ethylene species might be weakly adsorbed onto the CO-preadsorbed 80%Co/SiO_2 (with initial heat about 34 kJ/mol), which might be completely desorbed upon evacuation at 303 K. It should be mentioned that there were some di-σ-bonded ethylene formed upon the adsorption of C_2H_4 onto clean 80%Co/SiO_2 and 80%Co–8%ZrO_2/SiO_2.

3.6.4. Discussion of the adsorption of CO, H_2, and C_2H_4 onto cobalt

It is known that hydrogen atoms are adsorbed onto the three-fold hollow sites on cobalt surfaces [52,53], while CO molecules are adsorbed in bridged or linear forms onto cobalt. The adsorption of C_2H_4 onto clean cobalt surfaces led to the formation of surface ethylidyne and absorbed H atoms. Ethylene could also be bonded to a metal surface via a π or di-σ bond. These surface species are schematically depicted in Fig. 15. Apparently, the presence of adsorbed H atoms would not affect the adsorption of CO and C_2H_4 geometrically, and vice versa. On the other hand, the adsorption of CO and C_2H_4 would compete for the same surface cobalt sites.

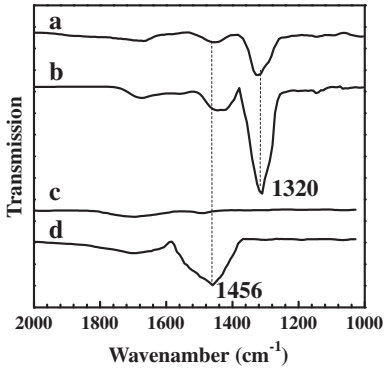

Fig. 14. Infrared spectra for the adsorption of ethylene at 303 K onto clean 80%Co/SiO_2 (a) and 80%Co–8%ZrO_2/SiO_2 (b) as well as onto CO-preadsorbed (C_2H_4/CO) 80%Co/SiO_2 (c) and 80%Co–8%ZrO_2/SiO_2 (d). The catalysts were reduced and evacuated at 773 K before the adsorption.

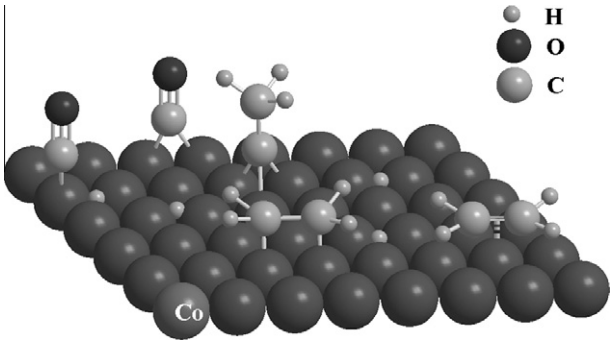

Fig. 15. Schematic diagram for the surface species from the adsorption of CO, H_2, and C_2H_4 onto the cobalt surface.

Fig. 15 shows the possible geometric interactions among the adsorbed surface species. The electronic effects among these surface species are much more complicated. The results of sequential adsorption of two probe molecules demonstrate such electronic interactions among the adsorbed species. For example, preadsorbed H atoms promote the adsorption of CO onto cobalt surface by enhancing the Co–CO bonding and CO coverage, while the preadsorbed CO inhibits the dissociative adsorption of ethylene. Adsorbed ethylene might be the basic unit for the propagation of carbon chains in FTS reactions. Thus, the dissociative adsorption of ethylene to form ethylidyne species was not desirable, since it might be the precursor of coke deposits. The results of sequential adsorption of CO and C_2H_4 suggested that the dissociative adsorption of ethylene would not occur on cobalt surfaces with preadsorbed CO. In addition, the nondissociative adsorption of C_2H_4 was significantly promoted by the presence of ZrO_2. In fact, while ethylene molecules might be adsorbed via π bonds onto the CO-preadsorbed 80%Co/SiO_2, they might be adsorbed via di-σ bonds onto the CO-preadsorbed 80%Co–ZrO_2/SiO_2. The di-σ-bonded C_2H_4 must be more easily activated than the π-bonded ones when they are incorporated into carbon chains during the chain propagation. That might be why the presence of ZrO_2 promoted selectivity to C_5^+ during the FTS reactions over Co/SiO_2 catalysts.

Thus, the presence of ZrO_2 in 80%Co–ZrO_2/SiO_2 performed multiple functions. It improved the dispersion of cobalt and thus increased the catalytic activity for FTS reactions. It promoted the adsorption of CO and H_2 and changed the adsorption state of C_2H_4 on cobalt surfaces with preadsorbed CO. All these functions were positive for the FTS reactions in terms of CO conversion and C_5^+ selectivity.

4. Conclusions

Adsorbed H, CO, and methylene (or molecularly adsorbed ethylene) on Co are usually taken as the primary surface species that react to form heavy hydrocarbons during FTS. Microcalorimetric adsorption and infrared spectroscopy were used in this work to determine the energetic interactions of these species with Co surfaces and their surface molecular structures, which were found to be affected by the presence of ZrO_2 as a promoter in Co/SiO_2. Specifically, ZrO_2 was found to promote the adsorption of H_2 (by enhancing the strength of Co–H bond) and CO (by increasing the uptake) on Co. In addition, it affected the co-adsorption of H_2, CO, and ethylene on Co. For example, the preadsorbed H significantly promoted the adsorption of CO and ethylene onto Co, and this promotion effect was enhanced by the presence of ZrO_2. While the adsorption of ethylene onto clean Co led to the formation of surface ethylidyne, which might cause coke deposition, such dissociative adsorption of ethylene was inhibited on Co when CO was co-adsorbed. In particular, ethylene was found to be mainly adsorbed via π and di-σ bonding on the CO-preadsorbed Co/SiO_2 and Co–ZrO_2/SiO_2, respectively. Such molecularly adsorbed ethylene molecules on Co are expected to favor chain propagation during Fischer–Tropsch synthesis. Thus, the presence of ZrO_2 strengthened the bonding of molecularly adsorbed ethylene and increased its uptake on Co with CO preadsorbed. This might be an important factor in the significantly higher selectivity to C_5^+ of Co/SiO_2 catalysts promoted with ZrO_2 during FTS. Based on the current experimental results, quantum calculations may be used to deepen understanding of the chain initiations and propagations on Co during the Fischer–Tropsch reactions.

Acknowledgments

Financial support from NSFC (20673055 and 21073089), MSTC (2005CB221400), and Jiangsu Province, China (BE2009145), is acknowledged.

References

[1] E. Iglesia, S.L. Soled, R.A. Fiato, J. Catal. 137 (1992) 212.
[2] E. Iglesia, Appl. Catal. A 161 (1997) 59.
[3] B. Ernst, S. Libs, P. Chaumette, A. Kiennemann, Appl. Catal. A 186 (1999) 145.
[4] I. Puskas, T.H. Fleisch, P.R. Full, J.A. Kaduk, C.L. Marshall, B.L. Meyers, Appl. Catal. A 311 (2006) 146.
[5] J.M. Jablonski, J. Okal, D. Potoczna-Petru, L. Krajczyk, J. Catal. 220 (2003) 146.
[6] J.S. Girardon, A.S. Lermontov, L. Gengembre, P.A. Chernavskii, A. Griboval-Constant, A.Y. Khodakov, J. Catal. 230 (2005) 339.
[7] Ø. Borg, J. Walmsley, R. Dehghan, B. Tanem, E. Blekkan, S. Eri, E. Rytter, A. Holmen, Catal. Lett. 126 (2008) 224.
[8] S. Krishnamoorthy, M. Tu, M.P. Ojeda, D. Pinna, E. Iglesia, J. Catal. 21 (2002) 422.
[9] S.L. Soled, E. Iglesia, R.A. Fiato, J.E. Baumgartner, H. Vroman, S. Miseo, Top. Catal. 26 (2003) 101.
[10] W. Ma, Y. Ding, L. Lin, J. Ind. Eng. Chem. 43 (2004) 2391.
[11] H. Xiong, Y. Zhang, K. Liew, J. Li, J. Mol. Catal. A 231 (2005) 145.
[12] D. Song, J. Li, J. Mol. Catal. A 247 (2006) 206.
[13] H. Zhao, J. Chen, Y. Sun, Stud. Surf. Sci. Catal. 147 (2004) 355.
[14] A.Y. Khodakov, W. Chu, P. Fongarland, Chem. Rev. 107 (2007) 1692.
[15] A. Jean-Marie, A. Griboval-Constant, A.Y. Khodakov, F. Diehl, C. R. Chim. 12 (2009) 660.
[16] A.Y. Khodakov, A. Griboval-Constant, R. Bechara, V.L. Zholobenko, J. Catal. 206 (2002) 230.
[17] G. Jacobs, T.K. Das, Y. Zhang, J. Li, G. Racoillet, B.H. Davis, Appl. Catal. A 233 (2002) 263.
[18] C.J. Bertole, C.A. Mims, G. Kiss, J. Catal. 221 (2004) 191.
[19] H. Xiong, Y. Zhang, K. Liew, J. Li, Fuel Process. Technol. 90 (2009) 237.
[20] E. van Steen, E.L. Viljoen, J. van de Loosdrecht, M. Claeys, Appl. Catal. A 335 (2008) 56.
[21] L.B. Shapovalova, G.D. Zakumbaeva, A.A. Zhurtbaeva, Stud. Surf. Sci. Catal. 147 (2004) 373.
[22] H. Chen, M. Xue, J. Shen, Catal. Lett. 135 (2010) 246.
[23] S. Hu, M. Xue, H. Chen, J. Shen, Chem. Eng. J. 162 (2010) 372.
[24] J. Gaube, H.F. Klein, J. Mol. Catal. A 283 (2008) 60.
[25] W.K. Hall, R.J. Kokes, P.H. Emmett, J. Am. Chem. Soc. 82 (1960) 1027.
[26] B.H. Davis, Catal. Today 141 (2009) 25.
[27] E. Iglesia, S.C. Reyes, R.J. Madon, J. Catal. 129 (1991) 238.
[28] J.M. Zowtiak, C.H. Bartholomew, J. Catal. 83 (1983) 107.
[29] F. Morales, E. de Smit, F.M.F. de Groot, T. Visser, B.M. Weckhuysen, J. Catal. 246 (2007) 91.
[30] R.C. Reuel, C.H. Bartholomew, J. Catal. 85 (1984) 63.
[31] A.Y. Khodakov, Catal. Today 144 (2009) 251.
[32] A.A. Khassin, T.M. Yurieva, G.N. Kustova, I.S. Itenberg, M.P. Demeshkina, T.A. Krieger, L.M. Plyasova, G.K. Chermashentseva, V.N. Parmon, J. Mol. Catal. A 168 (2001) 193.
[33] M.J. Heal, E.C. Leisigang, R.G. Torrington, J. Catal. 51 (1978) 314.
[34] M.J. Dees, T. Schidi, Y. Iwazawa, V. Ponec, J. Catal. 124 (1990) 530.
[35] K.R. Mohana, G. Spoto, A. Zecchina, J. Catal. 113 (1988) 466.
[36] K. Sato, Y. Inoue, I. Kojima, E. Miyajaki, I. Yasumori, J. Chem. Soc. Faraday Trans. I 80 (1984) 841.
[37] J. Zhang, J. Chen, J. Ren, Y. Sun, Appl. Catal. A 243 (2003) 121.
[38] S.T. Hussain, M. Mazhar, M.A. Nadeem, J. Nat. Gas Chem. 18 (2009) 187.
[39] M. Trépanier, A. Tavasoli, A.K. Dalai, N. Abatzoglou, Fuel Process. Technol. 90 (2009) 367.
[40] G. Calleja, A. De Lucas, R. Van Grieken, Appl. Catal. 68 (1991) 11.
[41] S. Bessell, Appl. Catal. A 126 (1995) 235.
[42] Y. Zhang, H. Xiong, K. Liew, J. Li, J. Mol. Catal. A 237 (2005) 172.
[43] R. Bouarab, O. Akdim, A. Auroux, O. Cherifi, C. Mirodatos, Appl. Catal. A 264 (2004) 161.
[44] T. López, R. Gomez, M.E. Llanos, E. López-Salinas, Mater. Lett. 38 (1999) 283.
[45] C.H. Bartholomew, R.J. Farrauto, J. Catal. 45 (1976) 41.
[46] M. Li, J. Shen, X. Ge, X. Chen, Appl. Catal. A 206 (2001) 161.
[47] M. Li, J. Shen, J. Catal. 205 (2002) 248.
[48] Y. Chen, Y. Chen, M. Gong, J. Zhou, Y. Zhang, J. Mol. Catal. China 7 (1993) 285.
[49] G. Blyholder, J. Phys. Chem. 68 (1964) 2772.
[50] J. Shen, J.M. Hill, R.M. Watwe, B.E. Spiewak, J.A. Dumesic, J. Phys. Chem. B 103 (1999) 3923.
[51] M. Li, J. Shen, W. Ji, Thermochim. Acta 345 (2000) 19.
[52] G.W. Watson, R.P.K. Wells, D.J. Willock, G.J. Hutchings, J. Phys. Chem. B 105 (2001) 4889.
[53] F. Zaera, Langmuir 12 (1996) 88.